Aerodynamic Characteristics of a NACA 4412 Airfoil

David Heffley

Mechanical Engineering Student
Baylor University

Dr. Kenneth Van Treuren

Mechanical Engineering Department
Baylor University

Abstract

The purpose of this experiment was to determine the lift and drag characteristics of the National Advisory Committee for Aeronautics (NACA) 4412 airfoil in a low speed wind tunnel. Previous airfoil experiments in the Baylor University wind tunnel resulted in discrepancies when compared to the published NACA data. Investigating these differences was the motivation for this series of experiments. Two methods were used to measure lift and drag on a 4412 airfoil; a force balance and a numerical integration of the surface pressure distribution. The calculated values were compared to the data published in NACA Reports 824 and 563. The experiment was conducted in a low speed, 24 by 24 inch wind tunnel. Two NACA 4412 airfoil models were used, one which mounted to a force balance and another with 18 pressure ported holes. Both airfoils were 24 inches wide and had a 6 inch chord length. All data were taken at a velocity of 50 ft/s, which is equivalent to a Reynolds number of 150,000 based on the airfoil chord length. The force balance data were taken at angles of attack (α) ranging from -8 to 20 degrees and the pressure data were taken from -18 to 20 degrees. Experimental lift coefficients at most non-stalled angles agreed within 2% of the NACA published data. Experimental drag coefficients when the airfoil was not stalled were as much as 130% different from the NACA data. Reasons for this high deviation in drag coefficients from the NACA data were investigated.

Keywords: Airfoil, NACA 4412, Low Speed Wind Tunnel, Pressure Distribution, Force Balance, Lift Coefficient, Drag Coefficient, Pressure Coefficient

Introduction

Significance

The lift and drag coefficients of an airfoil were studied in order to characterize the behavior of an airfoil at different angles of attack. The data was obtained from the Baylor University subsonic wind tunnel for possible student laboratory applications. Data from previous airfoil experiments at Baylor were inconsistent with the NACA data and no Baylor investigations to date have been as comprehensive as the current series of experiments. The data from this report will be used as a

reference for future low speed (low Reynolds number) airfoil data taken in the Baylor University wind tunnel. The experimental lift and drag coefficients were compared to the published NACA data for the 4412 airfoil. For NACA Report 563, NACA used a 54 port, 5 by 30 inch 4412 airfoil in a variable density wind tunnel at a Reynolds number of approximately 3,000,000 [1]. In NACA Report 824, NACA used a two foot chord, 4412 airfoil in a two-dimensional low-turbulence pressure tunnel and the drag was measured using the wake-survey method [2]. The current experiment used 24 inch 4412 airfoils with a 6 inch chord in the Baylor University low speed wind tunnel.

Theory

This experiment was carried out at 0.044 Mach (50 ft/s). The air was assumed to be incompressible. The viscous effects due to the surface of the airfoil at the test velocity were neglected because the surface of the airfoil was smooth. It was further assumed that the flow was along a streamline and steady. With these assumptions in place, Bernoulli's equation (Eq. 1) was used to find the dynamic pressure in the wind tunnel. This was done by using a Pitot-static tube. In Eq. 1, the dynamic pressure is equal to the difference in the total pressure and the static pressure. This is also equal to one half the density of air multiplied by the square of freestream velocity in the wind tunnel.

$$q = P_{Dyn} = P_{Total} - P_{Stat} = \frac{1}{2}\rho V_{\infty}^2 \qquad (1)$$

The first method used to calculate the lift and drag coefficients was a force balance. The lift force, L, and the drag force, D, were measured from the force balance and Eq. 2 and 3 were used to calculate the lift and drag coefficient. In Eq. 2 and 3, C_l is the coefficient of lift, C_d is the coefficient of drag, L and D are the lift and drag forces respectively, q or P_{Dyn} is the dynamic pressure from Eq. 1 and S is the planform area of the airfoil. The lift and drag directions are perpendicular and parallel to the freestream velocity represented by V_∞ in Fig. 1.

$$C_l = \frac{L}{qS} \qquad (2)$$

$$C_d = \frac{D}{qS} \qquad (3)$$

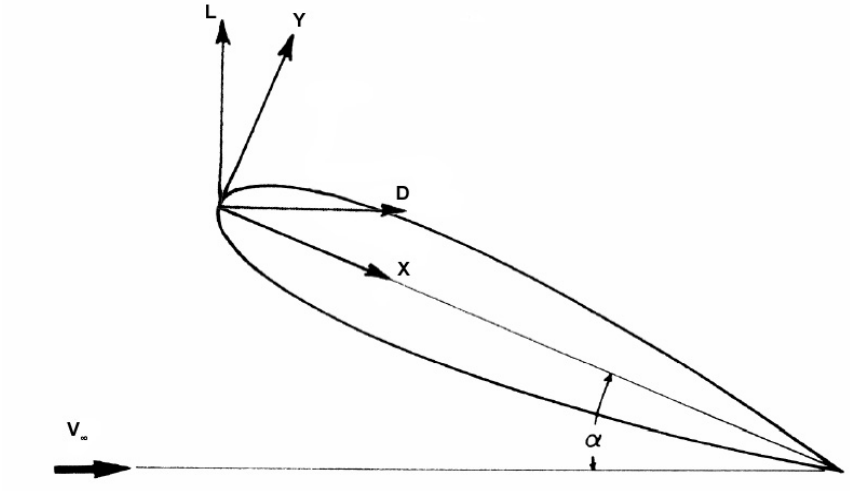

Figure 1. Axis Diagram

The second method used to calculate the lift and drag coefficients was the pressure distribution method. The first step of this method was to find the pressure coefficient at each point on the pressure ported airfoil. This was done by using Eq. 4.

$$C_P = \frac{P_{Local} - P_{Stat}}{q} \qquad (4)$$

In Eq. 4, C_P is the pressure coefficient, P_{Local}-P_{Stat} is the pressure difference between the local pressure port on the airfoil and the static pressure in the freestream, and q is the dynamic pressure of the freestream which is defined in Eq. 1. Once the pressure coefficient is calculated, the force coefficient in the X and Y direction can be calculated using the pressure coefficient at each point. The Y direction is always perpendicular to the chord while the X direction is parallel to the chord as seen in Fig. 1.

$$C_Y = \int_0^1 (C_{PL} - C_{PU}) d(\frac{x}{c}) \qquad (5)$$

$$C_X = \int_{-\frac{y}{c}}^{\frac{y}{c}} (C_{PF} - C_{PA}) d(\frac{y}{c}) \qquad (6)$$

C_Y and C_X are the force coefficients in the Y and X directions, C_{PL} and C_{PU} are the pressure coefficients on the lower and upper surface, and C_{PF} and C_{PA} are the pressure coefficients forward and aft of the point of maximum thickness on the airfoil. The force coefficients were found by numerically integrating using the trapezoidal rule.

$$C_Y = \left[\sum_{i=1}^{\infty} \left(\frac{(C_{Pi} + C_{Pi+1})}{2} \right) * \left| \frac{x_i}{c} - \frac{x_{i+1}}{c} \right| \right]_{Upper} - \left[\sum_{i=1}^{\infty} \left(\frac{(C_{Pi} + C_{Pi+1})}{2} \right) * \left| \frac{x_i}{c} - \frac{x_{i+1}}{c} \right| \right]_{Lower} \qquad (7)$$

$$C_X = \left[\sum_{i=1}^{\infty} \left(\frac{(C_{Pi} + C_{Pi+1})}{2} \right) * \left| \frac{y_i}{c} - \frac{y_{i+1}}{c} \right| \right]_{Front} - \left[\sum_{i=1}^{\infty} \left(\frac{(C_{Pi} + C_{Pi+1})}{2} \right) * \left| \frac{y_i}{c} - \frac{y_{i+1}}{c} \right| \right]_{Aft} \qquad (8)$$

Once the force coefficients were calculated, the lift and drag coefficients were found by using Eq. 9 and Eq. 10.

$$C_l = C_Y \cos\alpha - C_X \sin\alpha \qquad (9)$$

$$C_d = C_Y \sin\alpha + C_X \cos\alpha \qquad (10)$$

C_l and C_d are the force coefficients in the lift and drag directions as seen in Fig. 1. Furthermore, α is the angle of attack or the angle between the chord and the direction of airflow in the wind tunnel. All equations were obtained from Clancy [3] with the exception of Eq. 6 and 8 which were obtained from *Aerodynamic Forces on Airfoils* [4].

Equipment Employed

An Engineering Laboratory Design (ELD) Inc 24 inch Low Speed Wind Tunnel with an associated Wind Tunnel Instrumentation System was used in order to test the airfoils. An MKS Baratron 223B pressure transducer with a 10 port wafer switch was used to measure the dynamic and static pressures in the Pitot tube and on the pressure ported airfoil. Two separate NACA

4412 airfoils were used, one which was installed on to a force balance and another with 18 pressure ports which is inserted into the test section.

Calibration

The force balance dynamometer was the first piece of equipment to be calibrated. This force balance was calibrated according to the manufactures calibration procedures. The lift and drag were calibrated by using prescribed weights as recommended in the manufacturer's procedure. The pressure transducer was previously calibrated using a water monometer. Before every test, the drag, lift and pressure readouts were zeroed. For the pressure experiment, the port pressures were checked using the 10-port wafer switch on the MKS Baratron transducer to facilitate data acquisition. A protractor, which was used for both the force balance and the pressure ported airfoil to determine the angle of attack, was checked by making physical measurements of the airfoil's position and using geometry. The force balance airfoil was within 0.2 degrees of the angle protractor. However, on the pressure ported airfoil the angle was 0.5 degrees lower than the protractor measurement; this was taken into account at each angle tested.

Setup

To set up for the force balance method, the 4412 airfoil was secured to a force dynamometer which was then installed in the wind tunnel test section after calibration. The Pitot-static tube was then connected to the MKS Baratron pressure transducer. To analyze the pressure distribution, the 4412 pressure tapped airfoil was installed into the test section of the wind tunnel and connected to the MKS Baratron pressure transducer. During the experiment, as the airfoil's α increased, the airflow in the wind tunnel was restricted. In order to correct for this restriction in airflow, the fan speed was increased in order to keep the airflow at a constant 50 ft/s. This also kept the Reynolds number constant.

Velocity Testing

Velocities, ranging from 20 -100 ft/s, were initially tested to find the optimum velocity for the force balance and pressure distribution experiments. The velocity testing was accomplished because the NACA data contained a region of velocity (when the airfoil is not stalled) where the lift and drag coefficients are independent of the Re number. Two angles were tested, 0 and 6 degrees, to determine where the lift and drag coefficients were independent of the velocity. Fig. 2 illustrates how the lift coefficient is independent of the velocity from approximately 30 - 70 ft/s. The data for both tested angles indicate that at approximately 50 ft/s, the lift and drag coefficients were nearly independent of the velocity. Fig. 2 also illustrates how the flow is separated at low a velocity, which makes the coefficient of lift decrease significantly. This implies that the lift coefficient is not independent of the Re number at low velocities. At higher velocities the coefficient of lift gradually increases.

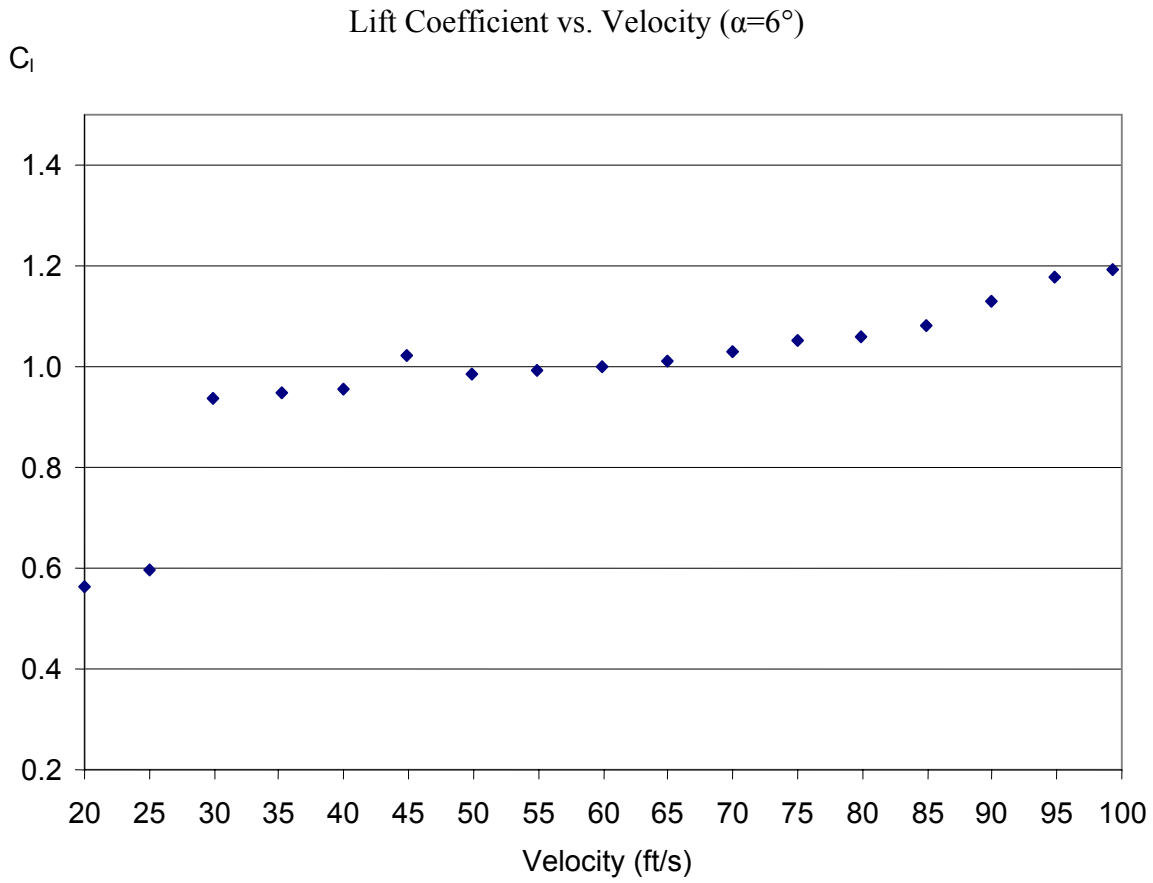

Figure 2. Velocity Testing

Procedure

At the start of every experiment the pressure and temperature in the room were recorded in order to determine the density of the air. The airflow velocity in the wind tunnel was then calculated using the density and the difference in static and total pressure (dynamic pressure) from the Pitot-static tube (see Eq. 1). A force balance was the first method used to find the lift and drag data. The force balance dynamometer was installed and data for the lift and drag were taken at 50 ft/s at angles ranging from -8 to 20 degrees at every degree. The second method used was the analysis of the pressure distribution which was found using the 18 port pressure airfoil. Data were taken at angles ranging from -18 to 20 degrees at every two degrees at angles below the stall region and at every degree at angles near or in the stall region. For each measured angle, a pressure value was extrapolated at the trailing edge to allow for a complete pressure distribution over the length of the chord. In all cases, five measurements of each variable were taken (lift, drag, Pitot-static pressure, and local pressure on the airfoil) and were averaged to reduce the uncertainty in the instrumentation. Once all of the data were collected, the lift and drag coefficients were calculated and compared with the published NACA data.

Results and Discussion

Force Balance Method

The force balance method yielded a lift coefficient graph which closely resembles the standard NACA data (see Fig. 3). In the current experiments, the airfoil stalled at a lower α than the NACA data because in this experiment the Reynolds number was around 150,000 compared to 3,000,000 for the NACA data. Data were not taken below -8 degrees because at angles below this angle the airfoil and force balance support violently shook making the lift and drag forces impossible to determine on the digital readout. The airfoil also shook at angles above 14 degrees, but not as violently as angles below -8 degrees. Therefore, reasonable data were obtained at a

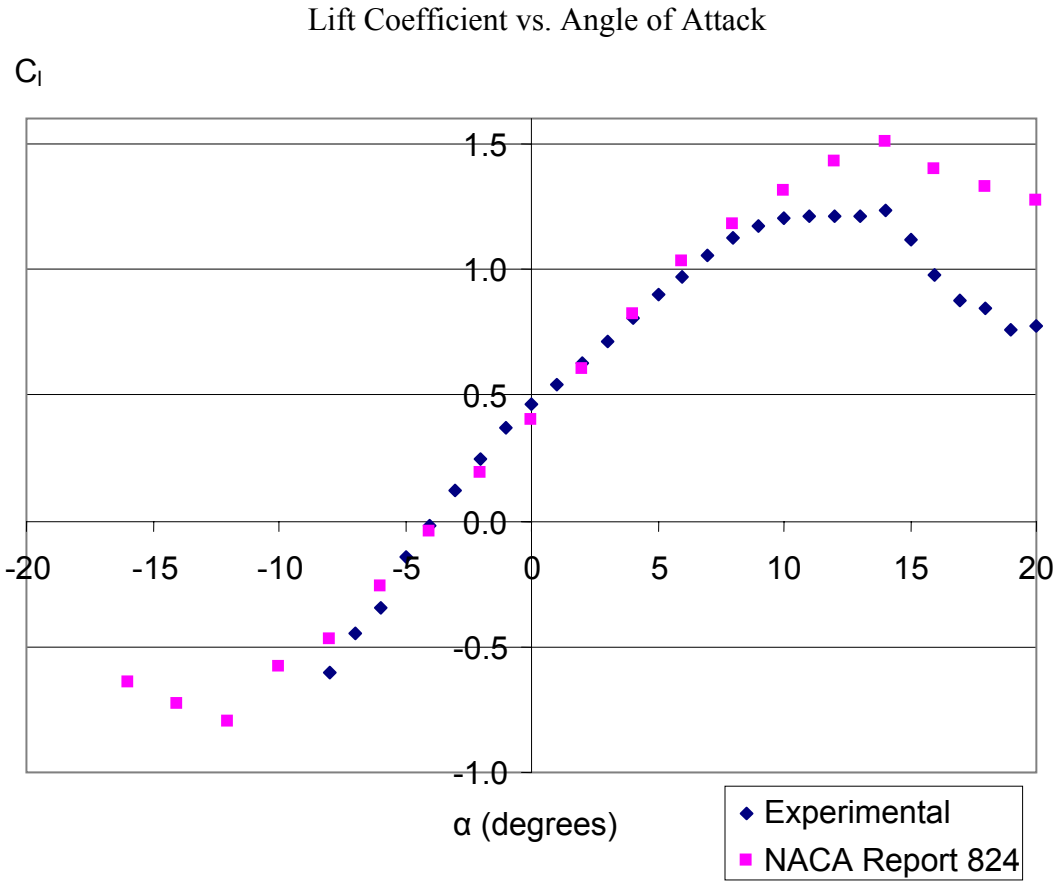

Figure 3. Force Balance Lift Coefficient

range of α from 14 - 20 degrees. The experimental drag coefficients were significantly different than the NACA data. The viscous effects on the surface of the airfoil were greater in this experiment due to a much lower Reynolds number compared to the NACA experiment. Another factor in the drag coefficient error is the tare value of the force balance support. The tare drag is the drag the force balance experiences without the airfoil. After the experiment, the tare value of the force balance support was tested. It was found that the support creates 0.0088 lb_f of tare drag. This along with the significantly lower Reynolds number contributes to the much higher drag coefficients.

Surface Pressure Distribution Method

Similar to the force balance method, the surface pressure distribution method yielded lift coefficient results closely related to the published NACA data. However, the drag coefficient results present a significant amount of differences. The experimental data follow the same linear pattern as the NACA report 563 data, but the stall in the current experiment occurs at a lower α due to the lower Reynolds number. The experimental drag coefficient is greater than the NACA drag coefficient and it is scattered. This is due to the unsteady pressure readings when the airfoil is stalled or close to stall. During the analysis of the data it was noticed that the pressure airfoil lacked a sufficient number of pressure ports in the front half of the airfoil to accurately calculate the drag coefficient using numerical integration. The arrows in Fig. 4 show the areas which are not included in the numerical integration, but are included in the NACA calculations. One can easily infer from this how the experimental data lacks enough data points to map out a similar shape as the NACA data. In contrast to Fig. 4, Fig. 5 illustrates the pressure distribution used to calculate the lift. In this case, the shape of the experimental graph and the NACA graph are

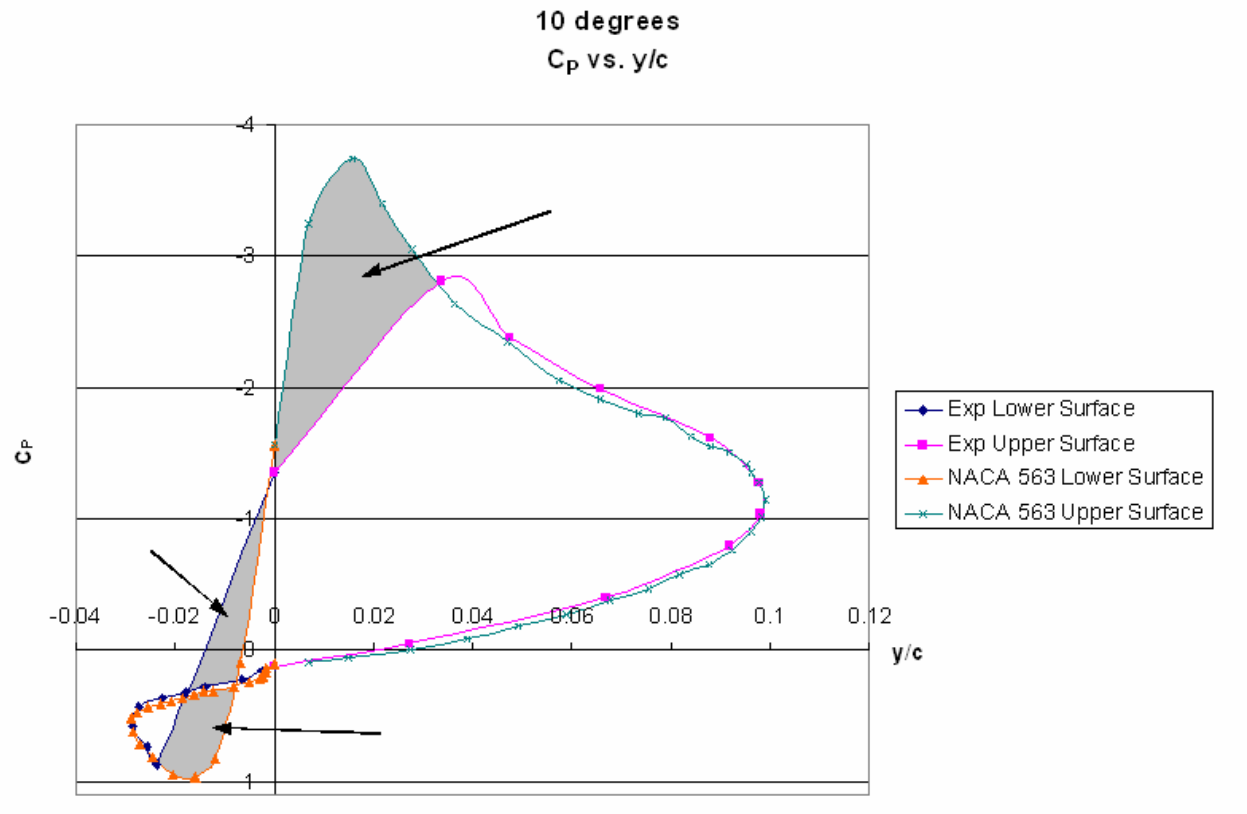

Figure 4. Pressure Distribution for Drag

similar, meaning there is no large area missing which numerical integration would not include. For this reason, the lift data was more accurate in the pressure distribution experiment than the drag data.

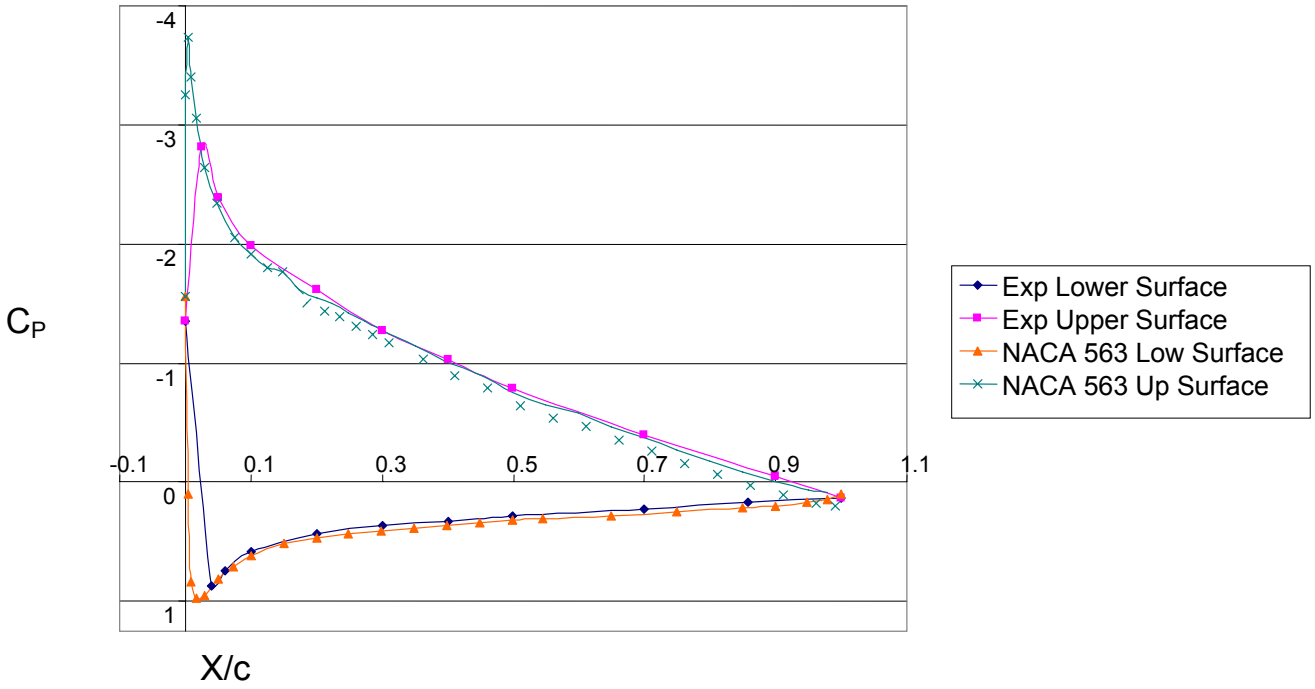

Figure 5. Pressure Distribution for Lift

Analysis of all Data

Both experimental methods, the force balance and the pressure distribution, worked very well in defining the lift coefficient versus angle of attack as seen in Fig. 6. To further illustrate the agreement between the experimental data and the NACA data, all of the data in the region where the airfoil was not stalled was compared using a linear trend line. It can be seen in Table 1 that the lift coefficients at all three example angles have a very low percent difference with the NACA data. However, the experimental drag coefficients were significantly different that the NACA drag coefficients, which can be seen in Table 2.

Table 1. Difference between Experimental C_l and NACA C_l

Coefficient of Lift (Percent Difference)	α (Degrees)	Experiment vs. 563 Data	Experiment vs. 824 Data
Force Balance	0.0	19.0%	15.4%
	4.0	2.0%	2.2%
	6.0	1.7%	6.1%
Pressure Distribution	0.0	2.2%	5.8%
	4.0	1.0%	3.1%
	6.0	1.5%	5.9%

Table 2. Difference between Experimental C_d and NACA C_d

Coefficient of Drag (Percent Difference)	α (Degrees)	Experiment vs. 563 Data	Experiment vs. 824 Data
Force Balance	0.0	89.1%	90.5%
	4.0	62.2%	94.2%
	6.0	46.0%	86.2%
Pressure Distribution	0.0	61.8%	63.4%
	4.0	105.4%	130.0%
	6.0	95.7%	126.8%

Airfoil theory suggests the lift curve slope is 2π, which is equivalent to about 0.1097/degree [3]. The slopes of each linear line in Figure 6 was calculated and compared to this theory and it was found that all of the data are within 12% of the theory.

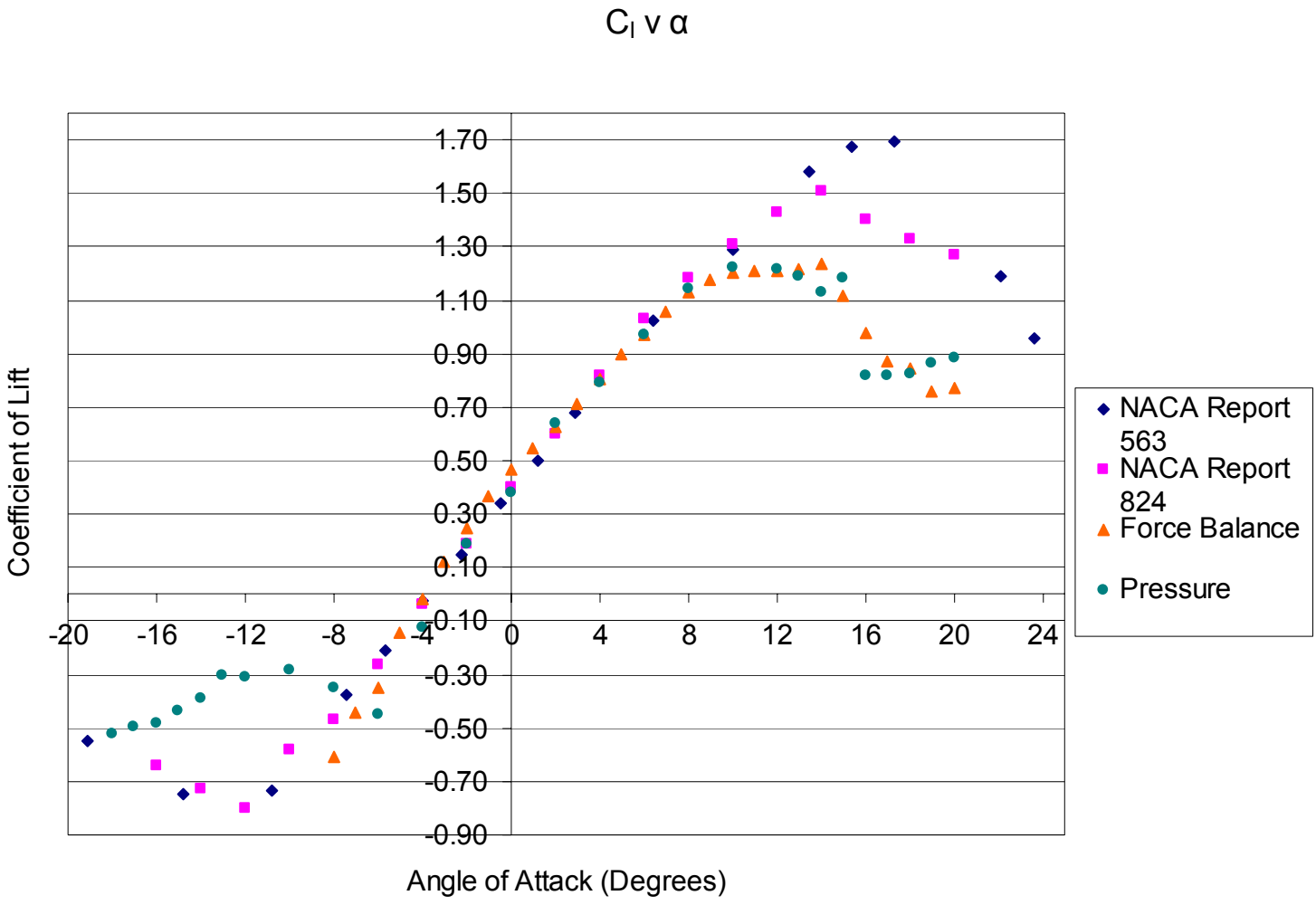

Figure 6. All Lift Coefficient Data Comparison

Experimental Error

The most noticeable experimental error occurred in reading the digital display for lift and drag from the force balance or the local pressure on the pressure airfoil near or beyond the stall angles. The force balance began to shake when it neared 14 degrees or -8 degrees. Data was not obtained beyond -8 degrees using the force balance because the lift and drag forces were so scattered the actual forces were not discernable. The pressure ported airfoil did not shake because it was fixed to the walls of the wind tunnel. However when the airfoil was stalled, the dynamic pressure reading from the Pitot-static tube had a wide range of readings. In some cases, especially at the extreme angles, this range was almost 15 percent of the average reading. Another source of error was the tare drag on the force balance support arm. After the experiment the force balance was recalibrated and tested in the wind tunnel without the airfoil. It was found that the drag on the support arm was 0.0088 lb_f, about 20 percent of the smallest drag reading and 0.8 percent of the highest drag reading. This tare value was not subtracted from the data because it was not discovered until the analysis of the force balance data was complete. The tare drag on the force balance has been noted and will be included as a bias in future Baylor wind tunnel experiments.

The most notable contribution to the discrepancy in the drag calculation for the experiment was the lack of a sufficient number of pressure ports on the pressure distribution airfoil to accurately calculate the lift and drag coefficients. From Fig. 4, it is easy to see how the NACA data points are more defined near the leading edge of the airfoil which results in more accurate data.

Another contribution to differences in calculations was the lack of pressure ports near the trailing edge of the airfoil. In order to numerically integrate for the lift and drag coefficients, a point was extrapolated at the trailing edge. This worked well when the airfoil was not stalled because the Kutta-condition was approximately satisfied. The Kutta-condition states that "the static pressure at the trailing edge on upper and lower (surfaces) is equal and thus the velocity vector is equal in magnitude and direction since in isentropic flow total pressure is constant" [5]. But as the airfoil was stalled, the trend of the data suggested that the Kutta-condition was not satisfied. There is no way to be certain because there are no pressure ports at the extreme trailing edge on the upper and lower surface of the airfoil.

It was determined that in this experiment the drag coefficient data could not accurately be compared to the NACA data due to the large difference of Reynolds numbers at which each experiment was completed (the NACA data was obtained at nearly 20 times the Reynolds number than the current experiment). The flow over the airfoil separates from the surface much sooner at lower Reynolds numbers. This will create a larger turbulent area in the wake of the airfoil increasing the pressure drag which in turn increases the total drag on the airfoil [6]. This is especially noticeable at higher angles of attack where the pressure drag is the dominate portion of the total drag. At an α near 0 degrees however, the lower Reynolds number accounts for an increase in viscous effects [7]. With a lower Reynolds number and small angles near 0 degrees, the airfoil in the experiment experienced a large viscous effect which increased the total drag. The airfoil section in Figure 7 shows how the drag coefficient is directly related to the Reynolds number. In general it portrays a decrease in drag coefficient with an increase in Reynolds number until it becomes approximately constant at a Reynolds number of $7x10^5$ Re.

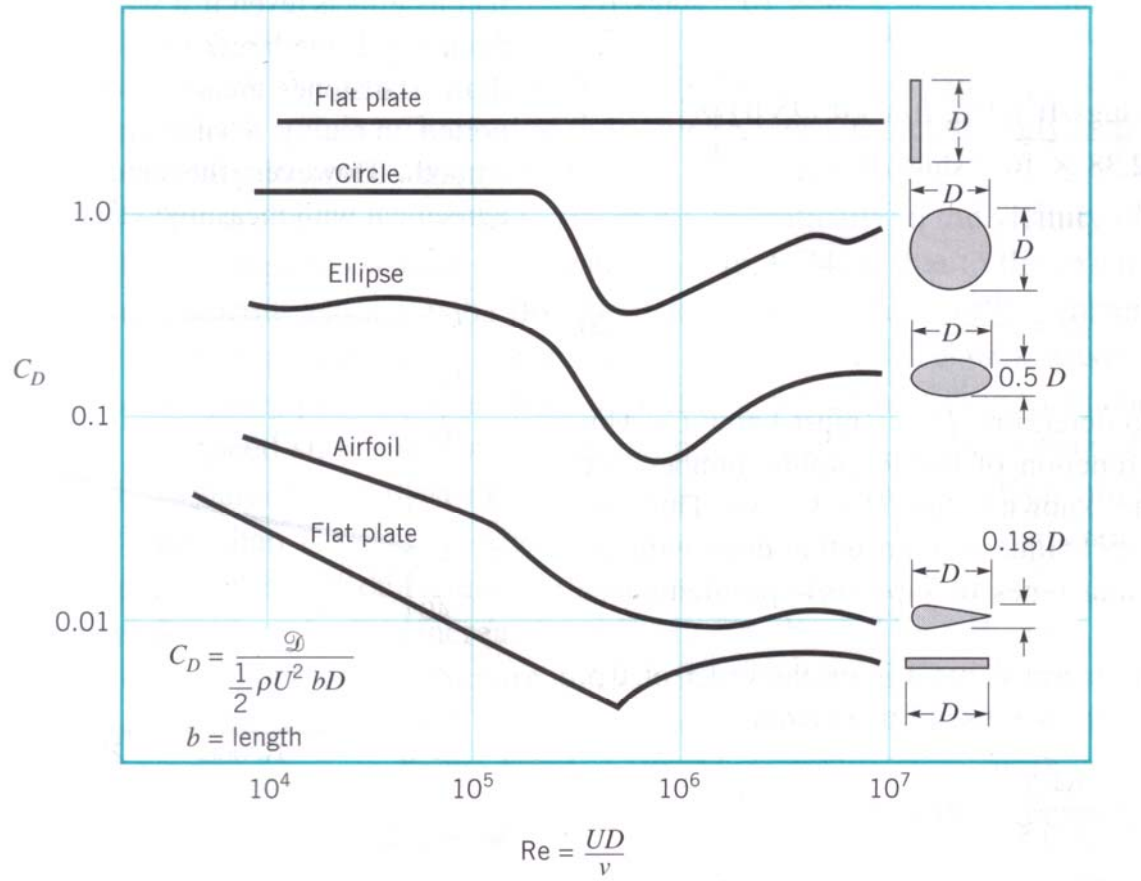

Figure 7. Drag Coefficient and Reynolds Number on an Airfoil [7]

Conclusions and Recommendations

In this experiment the lift and drag characteristics of a NACA 4412 airfoil were analyzed using a force balance and numerical integration of the pressure distribution. The lift coefficient calculated from these two methods agreed very closely with the two NACA reports (see Fig. 5 and 6). In contrast, the experimental drag coefficient for a given lift coefficient had a large percent difference with the published NACA data. This occurred because at a lower Reynolds number, 150,000 compared to 3,000,000 used for the NACA experiments, the viscous effects increase and therefore increase the total drag on the airfoil. This is true when the airfoil is at angles of attack near zero degrees or in the low drag regions. However, as the angle of attack is increased, most of the drag is due to the pressure drag on the airfoil while the viscous effects are negligible. This pressure drag increases as the Reynolds number decreases because the airflow separates closer to the leading edge which creates a larger turbulent region in the wake of the airfoil.

In future work, one could obtain drag data by using the wake-survey method. This could only be done at low angles in the Baylor University wind tunnel, but it would be interesting to see the differences between this method and the force balance and pressure distribution methods. One disadvantage in the experiment was the relatively few pressure ports at the leading and trailing

edge of the pressure airfoil. A more accurate pressure distribution over the airfoil could be obtained by creating a 4412 airfoil using stereo lithography or another type of 3D printing with more pressure ports near the leading and trailing edges. The drag coefficient data obtained using the pressure airfoil was unreliable and scattered for this very reason and more pressure ports would greatly enhance the accuracy of the data.

The NACA data was recorded at a much higher Reynolds number, around 3,000,000, than what was possible for this experiment. As a result, the drag data is significantly different and it can be concluded that drag must have some dependency on the Reynolds number. It was found that at a low α, the viscous effects were much greater because the Reynolds number was much less than the NACA experiment. The airflow at a high α separated earlier in this experiment because of the lower Reynolds number. This created a larger turbulent area behind the airfoil which increased the pressure drag and therefore increased the total drag. Furthermore, the pressure distribution method was determined to be inaccurate because the pressure ported airfoil being used lacked a sufficient number of pressure ports to accurately characterize the pressure distribution on the upper and lower surfaces.

The current experiment successfully concluded that NACA data will only agree with low speed wind tunnel lift coefficient data when the airfoil is not stalled. The NACA data will not agree with the drag coefficients obtained from a low speed wind tunnel due to the large difference in Reynolds number. It was further concluded that the previous airfoil experiments at Baylor University lacked a sufficient number of data points to accurately plot the lift and drag coefficients. The current experiment was much more comprehensive, obtaining over twice the amount of data. This allowed for a much more thorough experiment which could be compared to the NACA data with a much higher degree of confidence.

References

1. Pinkerton, R. M., 1937, "Calculated and Measured Pressure Distributions Over the Midspan Section of the NACA 4412 Airfoil," Report 563, NACA.
2. Abbott, I. H., Von Doenhoff, A. E., and Stivers, L. S. Jr., 1945, "Summary of Airfoil Data," Report 824, NACA.
3. L J Clancy, 1975, *Pitman Aeronautical Engineering Series*, John Wiley & Sons, Inc., pp. 54-115.
4. *Aerodynamic Forces on Airfoils*, http://www.aerospace.utoronto.ca/pdf_files/open_subsonic.pdf#search=%22open_subsonic%22, Date Accessed: August 26, 2006.
5. Schmidt, W., and Jameson, A., 2005, "Kutta Condition for Lifting Flows," Recent Advances in Numerical Methods in Fluids, 4, http://pc.freeshell.org/notes/node21.html.
6. Brandt, S. A., Randall, J. S., Bertin, J. J., and Whitford, R., 1997, *Introduction to Aeronautics: A Design Perspective*, American Institute of Aeronautics and Astronautics, Inc., Virginia, pp.78.
7. Munson, B. R., Young, D. F., and Okiishi, T. H., 2006, *Fundamentals of Fluid Mechanics*, 5th ed., John Wiley & Sons, Inc., New York, Appendix B, Chapter 9.